LAWRENCE
LIVERMORE
NATIONAL
LABORATORY

LLNL-JRNL-423533

Modeling Blood Flow in a Tilted IVC Filter: Does Tilt Adversely Affect Hemodynamics?

M. A. Singer, S. L. Wang

February 11, 2010

Journal of Vascular and Interventional Radiology

Disclaimer

Modeling Blood Flow in a Tilted IVC Filter: Does Tilt Adversely Affect Hemodynamics?

Authors: Michael A. Singer, PhD (1) and Stephen L.Wang, MD (2)

(1) Center for Applied Scientific Computing
Lawrence Livermore National Laboratory
Livermore, CA 94551

(2) Division of Vascular and Interventional Radiology
Kaiser Permanente Santa Clara
Santa Clara, CA 95051

ABSTRACT

Purpose:
Filter tilt is often seen with conical filters and adversely affects retrievability and clot trapping efficiency. In addition, tilt may also alter flow dynamics. This study uses computational fluid dynamics to evaluate flow past an unoccluded and partially occluded Celect inferior vena cava filter (Cook, Bloomington, IN). In particular, the hemodynamic response to thrombus volume and filter tilt is examined, and the results are compared to flow conditions known to be thrombogenic.

Materials and Methods:
Computer models of an upright and tilted Celect filter are constructed using high resolution digital photographs and methods of computer aided design. The three-dimensional models are placed inside a model cava, and steady-state flow past unoccluded and partially occluded filters is computed using the Overture software framework.

Results:
The volume of stagnant and recirculating flow increases with thrombus volume. In addition, as filter tilt increases, the cava wall in the direction of filter tilt is subjected to low velocity flow and gives rise to regions of low wall shear stress.

Conclusions:
Flow conditions caused by the tilted Celect filter may elevate the risk of intra/peri-filter thrombosis and facilitate vascular remodeling. This latter condition may increase the potential for incorporation of the hook of the filter into the vena cava wall, thereby complicating filter retrieval. These findings also suggest that further long-term clinical follow-up with conical filters should be pursued with a specific evaluation of tilt as a factor of intra-filter thrombus and thrombosis.

INTRODUCTION

Inferior vena cava (IVC) filters are a routine clinical treatment for the prevention of pulmonary embolism (PE) from deep vein thrombosis. An ideal IVC filter causes minimal disruption to the flow, effectively traps potential pulmonary emboli, is not inherently thrombogenic, is deployed through a low profile delivery system, and exhibits no long-term clinical complications. The PREPIC study group's 8 year follow-up of IVC filters versus anticoagulation alone demonstrated a decreased incidence of symptomatic PE in the filter group, but also noted a statistically significant increase in the incidence of DVT with the filter group (35.7% vs 27.5%, p=0.042) (1). These results have spawned interest in using retrievable IVC filters to prevent PE, particularly with prophylactic placement in patients with relatively short term risks for PE (e.g., trauma and surgical patients).

With conical, retrievable filters, including the G2 (Bard Peripheral Vascular, Tempe, AZ), the Gunther Celect, and the Gunther Tulip (Cook, Bloomington, IN), filter tilt is a common occurrence

and is often problematic when trying to retrieve the device (2-6). Retrieval of a tilted filter can be complicated by technically difficult engagement of the tip/hook with a snare due to position or angle, as well as a tip that is embedded into the cava wall.

The Gunther Celect filter is the second generation of the Gunther Tulip IVC filter. Built upon a similar conical design, the Celect utilizes four hooked primary legs and eight shorter, curved secondary legs. The secondary legs are designed to decrease the frequency and severity of tilt in comparison to the first generation Tulip filter. Recent studies on the Celect indicate the filter tilts greater than 5 degrees in approximately 33% of cases (7), and severe tilt (greater than 15-20 degrees) occurs in approximately 3-9% of cases (7-9).

With these relatively high rates of tilt, it is important to realize that clinical studies demonstrate attempted retrieval in only 26-50% of retrievable filters deployed; therefore, the majority of retrievable filters are left in-place as permanent filters (2-3, 10). Although the focus of recent studies on tilted filters has concentrated on tilt as a factor that complicates retrieval, this study aims to determine the impact of tilt on the hemodynamics inside the vena cava. In particular, if a large fraction of tilted filters become permanent filters, does tilt affect the risk of thrombosis? Does a tilted filter lead to hemodynamic conditions (e.g., stagnant and recirculating flow, abnormal wall shear stress (WSS) profiles) that may promote thrombosis?

Computational flow modeling has been used to study flow past IVC filters (11-13). However, all of these studies have evaluated filters in an ideal, centered position. In this study, we use computational fluid dynamics to evaluate the hemodynamics of an unoccluded and partially occluded Gunther Celect filter in non-tilted and tilted positions with particular interest in identifying regions of flow that elevate the risk of thrombogenesis.

MATERIALS AND METHODS

The Celect IVC filter (Fig. 1) is a low profile, retrievable, nitinol filter that has been retrieved from patients after being implanted for more than one year (14). Patients whose risk of pulmonary embolism decreases with time may be candidates for retrievable filters such as the Celect. Fig. 1a shows the real filter deployed in a glass test tube with an inner diameter of 23mm; Fig. 1b is the corresponding computer model.

The hook attached to the top of the filter allows retrieval of the Celect via a sheath inserted into the jugular vein. Fastening hooks at the end of the four straight legs (Fig. 1a) attach to the IVC and hold the filter in-place. The remaining eight curved legs are designed to support the filter and keep it centered in the vessel.

Computational models:

The IVC is modeled as a straight, rigid tube with an inner diameter of 23mm, per the average cava diameter described in Kaufman et al. (15). The length of the tube is 104mm, which provides adequate distance for the inlet velocity profile to develop fully before reaching the filter. Two overlapping grids are used to discretize the interior of the IVC: one high-resolution grid covers the inner boundary adjacent to the wall of the tube, and a second low-resolution grid fills the interior of

the tube. By using a high-resolution grid near the boundary of the IVC, adequate spatial resolution of the boundary layer is ensured, which is necessary for computing the WSS accurately.

A rigid, three-dimensional model of the Celect filter is constructed using the computer aided design features of the Overture software framework (16). The starting point for developing the model is a set of high-resolution digital photographs (e.g., Fig. 1a) that capture the filter in a glass test tube with a 23mm inner diameter (the same diameter as the model cava). The photographs are then imported into the GNU Image Manipulation Package where the filter geometry is extracted from pixel color and spatial coordinates. The data are then imported into Overture where the geometry is parameterized and a computational grid of the filter is constructed. Additional measurements of the filter (e.g., leg and tip sizes) are obtained using a digital caliper. The filter is discretized using approximately 50 body-fitted, overlapping grids. The spatial resolution of the grids is adjustable and is chosen to ensure adequate resolution of the flow throughout the entire domain (as determined by a grid resolution study, which is not shown here). The final computer model of the Celect filter is shown in Fig. 1b. Note that the model does not include the attachment hooks, which fasten the Celect to the IVC. Once deployed, these hooks become embedded in the vein and therefore do not obstruct the flow.

Thrombi are modeled as rigid spheres of 0.5mL and 1mL, which are representative of the volumes studied in-vitro by Wang et al. (17). In-vivo clots often assume random shapes with variable elasticity and porosity, but as noted by Swaminathan et al. (13), spherical models represent, in some sense, a statistical average of irregular shapes.

Blood is modeled as a homogeneous, incompressible, Newtonian fluid with density $\rho = 1040 kg/m^3$ and dynamic viscosity $\mu = 2.57e10^{-3} kg/(ms)$. From the work of Swaminathan et al. (13), the Newtonian approximation is appropriate for the current flow regime: non-Newtonian effects are minimal. The flow obeys conservation of mass and momentum as described by the incompressible Navier-Stokes (NS) equations (18). The single non-dimensional parameter that characterizes the flow is the Reynolds number, $Re = \rho UD/\mu$. Here, U is the mean inlet velocity, and D is the diameter of the tube.

As in (11), the three-dimensional NS equations are solved using the incompressible flow solver that is built upon the Overture software framework (19). Overture uses the method of overset grids to discretize partial differential equations on a collection of curvilinear meshes using finite difference approximations (20). This work uses second-order accurate spatial approximations and a steady-state flow solver. The solid walls of the pipe and filter are modeled as rigid, no-slip boundaries (i.e., zero velocity), and the inflow is specified by a parabolic inlet velocity profile with the axial component having a prescribed peak velocity; the transverse velocity components are zero.

All of the results presented here use a mean inlet velocity of U = 3.87cm/s, which corresponds to Re = 360. Previously published reports of vena cava simulations (e.g., [12, 21]) used similar Reynolds numbers. This Reynolds number corresponds to a blood flow rate of 0.96L/min in a 2.3cm vena cava, which is well within the range of 1.2 +/- 0.5L/min reported by Cheng et al. (22) for infrarenal flow at rest.

RESULTS

The three-dimensional NS equations are solved to determine the three components of velocity and the pressure. In all of the figures below, the flow is inferior-to-superior. Flow is modeled past the filter in three configurations: zero-tilt, where the tip of the filter is centered in the vein; half-tilt (7.5 degrees), where the tip is mid-way between the center and the left wall of the vein; and full-tilt (15 degrees), where the hook attached to the tip of the filter is touching the left wall of the vein. All three configurations are representative of clinical observations. The Celect is ideally positioned in the zero-tilt configuration.

The results below focus on the axial component of velocity, which is the dominant component. All wall shear stresses are plotted along two walls on opposite sides of the vessel and are in the plane of the tilted filter: the right cava wall, which is opposite the direction of tilt; and the left cava wall, which is in the direction of tilt, as illustrated in Fig. 1b. These two locations are chosen because they represent the extremes of WSS variations experienced by the vessel. That is, as the filter tilts, the right wall becomes the farthest wall from the filter tip, while the left wall becomes the closest. All velocities and wall shear stresses are normalized by the corresponding theoretical value for fully-developed flow in a long, straight pipe without a filter (i.e., Poiseuille flow) as in e.g., (11, 23-24).

Unoccluded filter:
Contour plots of the axial velocity are shown in Fig. 2. In all cases, the flow that enters the filter is fully developed. Flow with zero velocity is observed adjacent to all solid boundaries (i.e., IVC and filter), as expected from the no-slip boundary condition. Flow past the zero-tilt filter is nearly symmetric, with a region of low velocity flow surrounding the filter apex and hook. With increasing tilt, flow symmetry is broken, and the volume of stagnant flow surrounding the filter apex and hook increases due to a larger filter cross-section that is exposed to on-coming flow. For the case of full-tilt, a large region of stagnant flow is observed near the wall of the vessel, and low velocity flow is observed between the hook and the leg that touches the vein. These regions of slow flow may promote the accumulation of platelets. The peak normalized velocity, which occurs inside the filter, also increases with filter tilt (2.06, 2.15, and 2.26 for 0, 7.5, and 15 degrees of tilt, respectively), but the minimum velocities remain virtually unchanged.

The WSS for the right and left cava walls becomes increasingly different with filter tilt (Fig. 3). On the right wall, the peak WSS decreases with filter tilt as the apex of the filter moves away from the wall and allows flow to pass through a wider opening thereby weakening the velocity gradient near the wall. Upstream of peak, the WSS drops below the free-stream value due to momentum loss caused by the filter leg near the wall. The WSS nearly returns to its free-stream value at the outflow.

The left cava wall experiences flow disruption due to filter tilt (Fig. 3). As tilt increases, so does the peak WSS, which is located between the hook and leg/wall intersection. For the case of full-tilt, the flow immediately upstream and downstream of the hook is nearly stagnant (i.e., Fig. 2c), which leads to near-zero WSS. These two regions of low WSS, which become more pronounced with tilt, may facilitate the accumulation of platelets. In addition, the close proximity of the hook

to the cava wall elevates the risk of cava damage (e.g., perforation [25]), which further increases the risk of thrombosis and complicates retrieval.

Partially occluded filter:
Flow past the partially occluded Celect filter with 0.5mL and 1mL spherical thrombus is shown in Fig. 4 and Fig. 5, respectively. In both cases, the zero-tilt configuration exhibits stagnant flow downstream of the thrombus and hook, and disrupted flow is confined to the center of the vessel. As tilt and thrombus size increase, however, the volume of disrupted flow also increases, and a region of stagnant flow develops along the wall of the vessel. For the1mL thrombus with full-tilt, flow disruption along the vessel wall persists well downstream of the filter, thereby providing hemodynamic conditions that may be thrombogenic. Maximum axial velocities increase with tilt and thrombus volume; the minimum axial velocities also increase, which indicates a decrease in the strength of flow reversal as flow is pushed around the thrombus with greater velocity.

The peak WSS along the right cava wall decreases with filter tilt and increases with thrombus volume (Figs. 6-7). The former trend is due to a widening gap between the vessel wall and the clot, which results in lower velocity gradients in the boundary layer. Conversely, the larger thrombus provides a narrower passage between the vessel wall and the thrombus, which results in higher flow velocities past the thrombus in order to maintain conservation of mass. For both volumes of thrombus, a decrease in WSS is observed near the upstream contact point of the filter leg and vessel wall; this is a region of low velocity flow. In all cases, the WSS far downstream of the filter nearly returns to its unperturbed upstream value, which indicates that the disruption of the WSS due to the filter is localized.

Wall shear stress profiles for both thrombi are qualitatively similar. However, the magnitude of the peak WSS increases with volume (similarly for axial velocity), while the minimum wall shear stresses remain virtually identical. In addition, the length of the left cava wall that is exposed to low, normalized WSS (e.g., < 1) increases with tilt (both upstream and downstream of peak), but remains nearly constant for both sizes of thrombus.

DISCUSSION

The relationship between filter tilt and trapping efficacy for conical filters has been evaluated in both clinical and in-vitro studies; however, most studies were performed on early IVC filter designs including the Greenfield, Simon Nitinol, and Modin-Uddin filters (26-28). These studies primarily evaluated the effect of filter tilt on the ability to trap clots, and the results demonstrated that tilted conical filters generally trap smaller clots less efficiently than centered conical filters (26, 28). More recent in-vitro studies on the Gunther Tulip and Celect filters demonstrated a decrease in trapping efficiency of smaller simulated thrombi as tilt increases (29). This phenomenon is presumed to be due to a tilted conical filter allowing more clots to pass through it as an eccentric, tilted filter allows more IVC cross section to be unfiltered (26).

Although clot trapping efficiency is important when evaluating the performance of tilted filters, our results show that tilt also alters the hemodynamic response of blood flow. Further, the flow disruption caused by tilt is critical for determining the efficacy of filters, and using computational

flow simulations to model the hemodynamic effects of tilt is ideal because it obviates the need for time-consuming and expensive bench experiments. Moreover, modifying parameters such as the degree of tilt, volume and location of trapped thrombi, and inflow flow speed is seamlessly accomplished in the computer model. Computational flow modeling has been used to evaluate filter flow conditions, but previous studies have focused exclusively on optimally centered IVC filters (11-13). This work represents the first modeling study that analyzes the hemodynamic response to tilted filters.

Our model is based on simplified, but mostly realistic assumptions of the IVC and trapped thrombus. Although flow through the IVC is mildly pulsatile (in comparison, for example, to aortic flow) and affected by respiration, for simplicity the model assumes the flow is steady-state, and the prescribed flow rate is set to be within the range of normal infrarenal inflow at rest (22). The walls of the model IVC are taken to be smooth and rigid, and inflow into the IVC from other veins including the renal, lumbar, and iliac veins is not evaluated. Thrombi are also modeled as rigid spheres.

The figures above indicate that the volume of stagnant and recirculating flow increases with tilt and thrombus volume. In particular, low velocity flow is observed near the apex of the filter (e.g., tip and hook) and immediately downstream of all thrombi. For the zero-tilt configuration, these abnormal flow patterns are located in the center of the vessel and away from the vessel walls, thereby minimizing the volume of stagnant/recirculating flow along the wall of the IVC. As tilt increases, however, the tip and hook of the filter move closer to the vessel wall, which exposes the vessel to slow, stagnant and recirculating flow with a longer residence time than the zero-tilt configuration. These regions of stagnant and recirculating flow, combined with low shear stress, have been shown to be thrombogenic (30-32). In particular, the cava wall in the direction of filter tilt is especially prone to platelet deposition and accumulation, and the risk of thrombosis increases, particularly for the partially occluded filter. Further, stagnation zones may allow thrombin and fibrin to accumulate and initiate secondary hemostasis. Given that the majority of retrievable filters deployed ultimately become permanent filters, the long-term risks of thrombosis from either trapped thrombus or regions that support inherently thrombogenic flow conditions carries significant clinical importance.

The Celect IVC filter is relatively new to market and large, long-term studies are lacking on the incidence of cava occlusion or significant intra-filter thrombus. Lyon et al. noted 0% incidence of caval occlusion at retrieval of 58 patients and intra-filter thrombus in 7% (n=4) with a mean indwell time of 179 days (7). Dey et al. noted significant clot in the filter at retrieval in 8% of patients (3 out of 38) with a mean indwell time of 71 days (33). However, evaluating our results, which represent the typical hemodynamic response of conical filters in general, suggests that the majority of the flow disturbances from partially occluded filters are generated by the trapped thrombi and not the filter itself. In this sense, all tilted conical filters, including the Bard G2, Cook Tulip, Rex Medical Option IVC, and the ALN filters, are susceptible to flow conditions that increase the risk of thrombosis. Many long-term studies on the Celect's predecessor, the Gunther Tulip, have been published. In these studies, IVC occlusion rates are reported to be 0-2.4%, and rates of non-occlusive trapped thrombus (sometimes large) are reported to be 0.7-14% (2, 3, 10, 34-36). However, data that correlate filter tilt with thrombus and thrombosis is limited. Sag et al. notably described that filter tilt did not impair the Tulip's ability to prevent PE; however, the study did note

that “the 25 filters with trapped thrombus had substantial frequency and magnitude of tilt at the first retrieval attempt. These data may be interpreted to mean that Gunther Tulip Filter may be effective at trapping clot with the reported tilt magnitude. However, an alternative explanation is the filter tilt results in a thrombogenic flow disturbance resulting in thrombus formation within the filter” (35). This latter explanation is consistent with our findings, and further long-term clinical studies that evaluate tilt of conical filters as a factor of IVC occlusion and intra-filter thrombus frequency should be pursued.

Our flow modeling study suggests that thrombi trapped in the apex of tilted filters may facilitate the formation of a thrombogenic state along the cava wall. The hemodynamic response to thrombus trapped along the wall was previously studied using flow models and in-vitro experiments (11, 24). In particular, these studies examined the upstream trapping position of the TrapEase and OptEase filter, where thrombi are caught along the cava wall are was found to be potentially thrombogenic (11, 24). In addition to stagnant and recirculating flow, WSS is also an important clinical consideration because dissolution of thrombi increases with WSS (12). That is, when wall shear stresses are sufficiently high, trapped thrombus are subjected to shear stresses that reduce thrombus volume by thrombolysis. As the Celect filter increases tilt, thrombi are trapped closer to the vessel wall, and the flow pattern is reminiscent of a TrapEase or OptEase filter with thrombus in the upstream trapping position (11). Consequently, the stagnant/recirculating zones and corresponding regions of low WSS inhibit dissolution and, as noted by Stewart et al., may promote continued aggregation of blood elements, clot growth, and intimal hyperplasia (12). It is also recognized by other computational and in-vitro studies (11, 12, 23, 37) that capturing thrombus next to the cava wall is not optimal and should be avoided.

Several clinical papers have evaluated the technical reasons for failed or difficult conical filter retrieval with the most common factors including: severe tilt, filter hook opposing the cava wall, adherent thrombus at the hook site, and hook embedded into the cava wall (4-6, 38). Many cases have been described of significantly tilted conical filter tips that develop endothelial caps at the contact site with the cava wall. Our flow modeling study of the tilted Celect filter sheds light on the potential mechanistic properties involved. The formation of intimal hyperplasia and the remodeling of smooth muscle cells have been linked to regions of low WSS and high WSS gradients (39, 40). Consequently, an IVC filter that promotes these hemodynamic effects, especially when tilted, is more likely to generate conditions conducive to endothelialization. As observed above, when the Celect is fully tilted, it induces regions of low WSS along the left cava wall near the tip and hook of the filter, and the length of cava wall that is exposed to low WSS increases with thrombus volume. These regions of the vessel are therefore at elevated risk of abnormal migration and growth of smooth muscle cells, which may ultimately lead to vessel remodeling and endothelialization of the filter tip.

In summary, our computational model of flow past a tilted Celect IVC filter with and without non-occlusive thrombi demonstrates areas of low wall shear stress and stagnant/recirculating flow along the cava wall in the direction of tilt. These areas demonstrate characteristics that are potentially thrombogenic and may lead to conditions that favor vascular endothelialization of the filter tip. One clinical study that specifically evaluated the tilt of a conical filter noted that, among filters with trapped thrombus, there was a high degree and frequency of filter tilt and that filter tilt may lead to a thrombogenic state (35). With the increasing use of retrievable filters and the fact that most

retrievable filters become permanent filters, further large-scale and long-term studies of filter tilt as a factor of IVC thrombosis and non-occlusive filter thrombus need to be performed. With more convincing future clinical data, intervention for severely tilted filters may need to be performed at the time of placement or shortly thereafter.

ACKNOWLEDGEMENTS

MAS is grateful for the assistance of Dr. William Henshaw. Computer time on LLNL's Yana cluster was provided under Livermore Computing's Multiprogrammatic & Institutional Computing Initiative. LLNL is operated by Lawrence Livermore National Security, LLC, for the DOE, National Nuclear Security Administration under Contract DE-AC52-07NA27344.

REFERENCES

1. The PREPIC Study Group. Eight year follow-up if patients with permanent vena cava filters in the prevention of pulmonary embolism. Circulation 2005; 112:416-422.

2. Smouse HB, Rosenthal D, Van Ha TG, et al. Long-term retrieval success rate profile for the Gunther Tulip vena cava filter. J Vasc Interv Radiol 2009; 20:871-877.

3. Ray CE, Mitchell E, Zipser S, et al. Outcomes with retrievable inferior vena cava filters: a multicenter study. J Vasc Interv Radiol 2006; 17:1595-1604.

4. Stavropoulos SW, Dixon RG, Burke CT, et al. Embedded inferior vena cava filter removal: use of endobronchial forceps. J Vasc Interv Radiol 2008; 19:1297-1301.

5. Van Ha TG, Vinokur O, Lorenz J, et al. Techniques used for difficult retrievals of the Gunther Tulip inferior vena cava filter: experience in 32 patients. J Vasc Interv Radiol 2009; 20:92-99.

6. Lynch F. Balloon-assisted removal of tilted inferior vena cava filters with embedded tips. J Vasc Interv Radiol 2009; 20:1210-1214.

7. Lyon SM, Riojas GE, Uberoi R, et al. Short- and long-term retrievability of the Celect vena cava filter: results from a mulit-institutional registry. J Vasc Interv Radiol 2009; 20:1441-1448.

8. Rosenthal D, Kochpura PV, Wellons ED, et al. Gunther Tulip and Celect IVC filters in multiple trauma patients. J Endovasc Ther 2009; 494-499.

9. Sangwaiya MJ, Marentis TC, Walker G, et al. Safety and effectiveness of the Celect inferior vena cava filter: preliminary results. J Vasc Interv Radiol 2009; 20:1188-1192.

10. Karmy-Jones R, Jurkovich G, Velhamos GC, et al. Practice patterns and outcomes of retrievable vena cava filters in trauma patients: an AAST multicenter study. J Trauma 2007; 62:17-25.

11. Singer MA, Henshaw WD, Wang SL. Computational modeling of blood flow in the TrapEase inferior vena cava filter. J Vasc Interv Radiol 2009; 20:799-805.

12. Stewart SF, Robinson RA, Nelson RA, Malinauskas RA. Effects of thrombosed vena cava filters on blood flow: Flow visualization and numerical modeling. Ann Biomed Eng 2008; 36(11):1764-1782.

13. Swaminathan TN, Hu HH, Patel AA. Numerical analysis of the hemodynamics and embolus capture of a Greenfield vena cava filter. J Biomed Eng 2006; 128:360-370.

14. Doody O, Noe G, Given MF, et al. Assessment of snared-loop technique when standard retrieval of inferior vena cava filters fails. Cardiovasc Intervent Radiol 2009; 32(1):145-149.

15. Kaufman JA, Waltman AC, Rivitz SM, Geller SC. Anatomical observations on the renal veins and inferior vena cava at magnetic resonance angiography. Cardiovasc Intervent Radiol 1995; 18:153-157.

16. https://computation.llnl.gov/casc/Overture/

17. Wang SL, Timmermans HA, Kaufman JA. Estimation of trapped thrombus volumes in retrievable inferior vena cava filters: A visual scale. J Vasc Interv Radiol 2007; 18:273-276.

18. Batchelor GK. An introduction to fluid dynamics. Cambridge University Press, Cambridge, UK 1980.

19. Henshaw WD. Cgins: A solver for the incompressible Navier-Stokes equations on composite overlapping grids. LLNL Technical Report 2008, LLNL-SM-403631.

20. Chesshire GS, Henshaw WD. Composite overlapping meshes for the solution of partial differential equations. J Comp Phys 1990; 90(1):1-64.

21. Rahbar E, Moli D, Moore J. Three-dimensional analysis of flow disturbances from clots in vena cava filters. J Vasc Interv Radiol 2009; 20(2):S22.

22. Cheng CP, Herfkens RJ, Taylor CA. Inferior vena cava hemodynamics quantified in vitro at rest and during cyclic exercise using magnetic resonance imaging. Am J Physiol Heart Circ Physiol 2003; 284:1161-1167.

23. Leask RL, Johnston KW, Ojha M. In vitro hemodynamic evaluation of a Simon Nitinol vena cava filter: Possible explanation of IVC occlusion. J Vasc Interv Radiol 2001; 12:613-618.

24. Leask RL, Johnston KW, Ojha M. Hemodynamic effects of clot entrapment in the TrapEase inferior vena cava filter. J Vasc Intervent Radiol 2004; 15:485-490.

25. Sadif A, Rasuli P, Olivier A, et al. Significant caval penetration by the Celect inferior vena cava filter: Attributable to filter design. J Vasc Interv Radiol 2007; 18:1447-1450.

26. Katsamouris AA, Waltman AC, Delichatsios MA, et al. Inferior vena cava filters: in vitro comparison of clot trapping and flow dynamics. Radiology 1988; 166:361-366.

27. Kinney TN, Rose SC, Weingarten KE, et al. IVC filter tilt and asymmetry: comparison of the over-the-wire stainless- steel and titanium Greenfield IVC filters. J Vasc Interv Radiol 1997; 8:1029-1037.

28. Palestrant AM, Prince M, Simon M, et al. Comparative in vitro evaluation of the nitinol inferior vena cava filter. Radiology 1982; 145:351-355.

29. Gunther RW, Neurburg J, Mossdorf A, et al. New optional IVC filter for percutaneous retrieval: in vitro evaluation of embolus capturing efficiency. Rofo 2005; 177:632-636.

30. Folie BJ, McIntire LV. Mathematical analysis of mural thrombogenesis. Biophys J 1989; 56:1121-1141.

31. Davies PF. Hemodynamic shear stress and the endothelium in cardiovascular pathophysiology. Nat Clin Pract Cardiovasc Med 2009; 6:16-26.

32. Lowe G. Virchow's triad revisited: abnormal flow. Pahtophysiol Haemost Thromb 2004; 33:455-457.

33. Dey C, Al-Humayyd S, Valenti DA. Retrievability of the Celect vena cava filter [abstract]. In: Annual Meeting of the Society of Interventional Radiology; 2009 Mar 7-12; San Diego, CA. SIR; 2009. p S23. Abstract nr 55.

34. Hoppe H, Nutting CW, Smouse R, et al. Gunther tulip filter retrievability multicenter study including CT follow-up: final report. J Vasc Interv Radiol 2006; 17:1017-1023.

35. Sag AA, Stavas JM, Burke CT, et al. Analysis of tilt of the Gunther Tulip filter. J Vasc Interv Radiol 2008; 19:669-676.

36. Millward SF, Oliva VL, Bell SD, et al. Gunther Tulip retrievable vena cava filter: results from the Registry of the Canadian Interventional Raidology Association. J Vasc Interv Radiol 2001; 12:1053-1058.

37. Harlal A, Ojha M, Johnston, KW, Vena cava filter performance based on hemodynamics and reported thrombosis and pulmonary embolism patterns. J Vasc Interv Radiol 2007; 18:103-115.

38. Marquess JL, Burke CT, Beecham AH, et al. Factors associated with failed retrieval of the Gunther Tulip inferior vena cava filter. J Vasc Interv Radiol 2008; 19:1321-1327.

39. Keynton RS, Evancho MM, Sims RL, et al. Intimal hyperplasia and wall shear in arterial bypass graft distal anastomoses: An in-vivo model study. J Biomech Eng 2001; 123:464-473.

40. Wang HQ, Huang LX, Qu MJ, et al. Shear stress protects against endothelial regulation of vascular smooth muscle cell migration in a coculture system. Endothelium 2006; 13:171-180.

CONFLICT OF INTEREST STATEMENT

The authors declare no conflicts of interest.

FIGURES

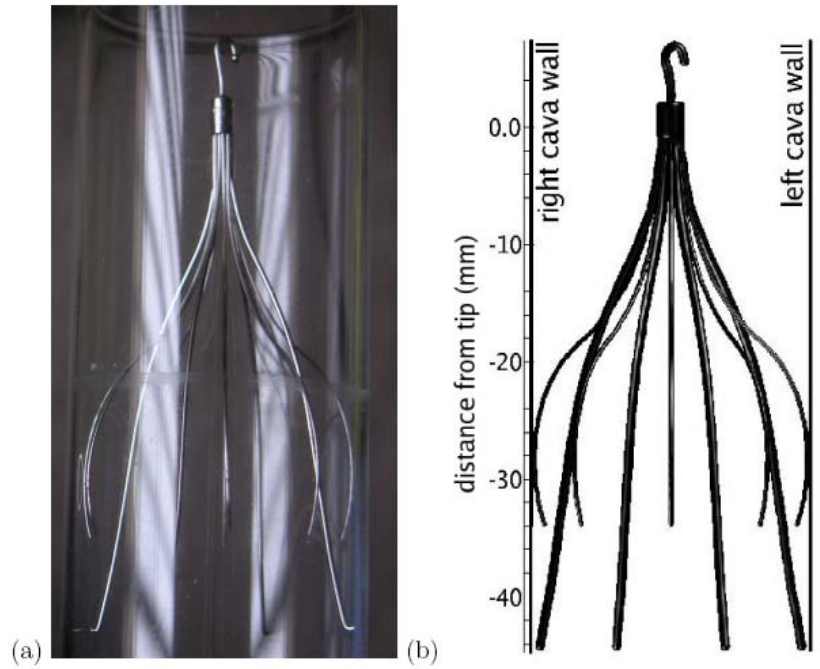

Figure 1: Celect filter: (a) real filter in a glass test tube with a 23mm inner diameter; (b) three-dimensional computer model sized to fit the same tube.

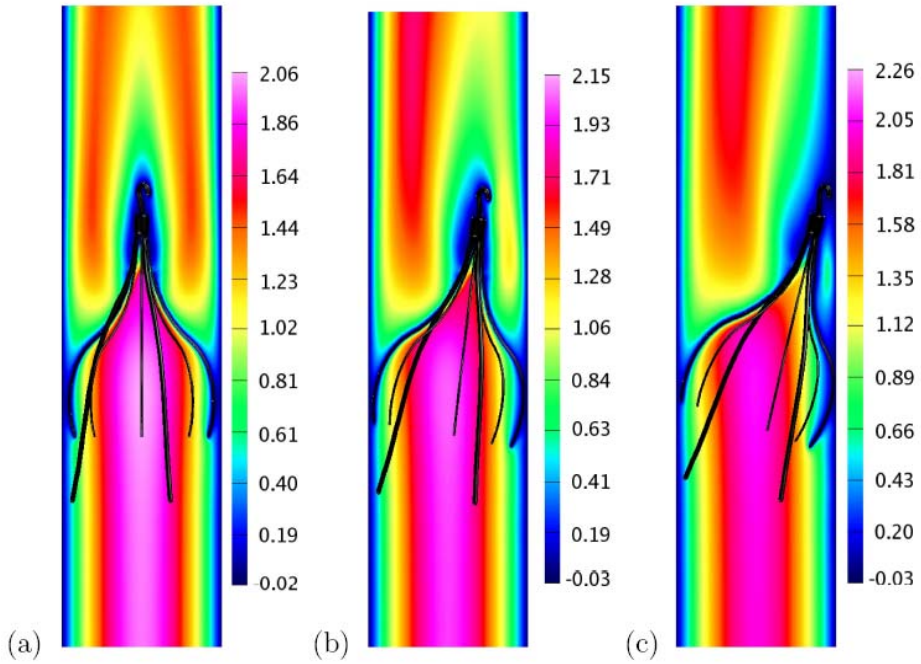

Figure 2: Axial velocity contours for the unoccluded Celect filter: (a) zero-tilt; (b) half-tilt (7.5 degrees); (c) full-tilt (15 degrees).

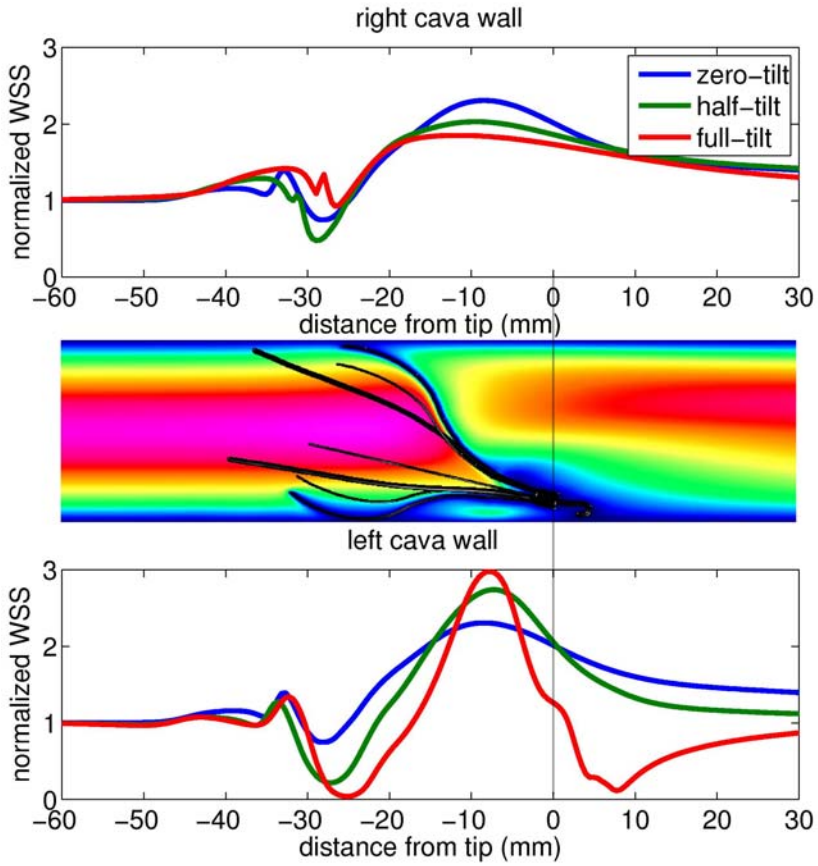

Figure 3: Wall shear stress for the unoccluded Celect filter: right cava wall (top); left cava wall (bottom).

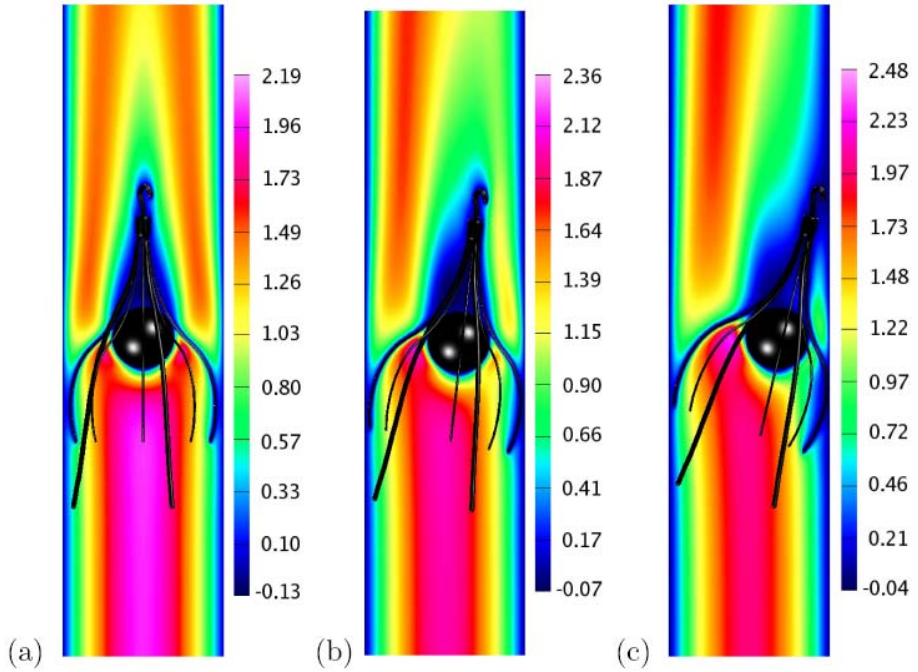

Figure 4: Axial velocity contours for the partially occluded Celect filter with a 0.5mL spherical clot: (a) zero-tilt; (b) half-tilt (7.5 degrees); (c) full-tilt (15 degrees).

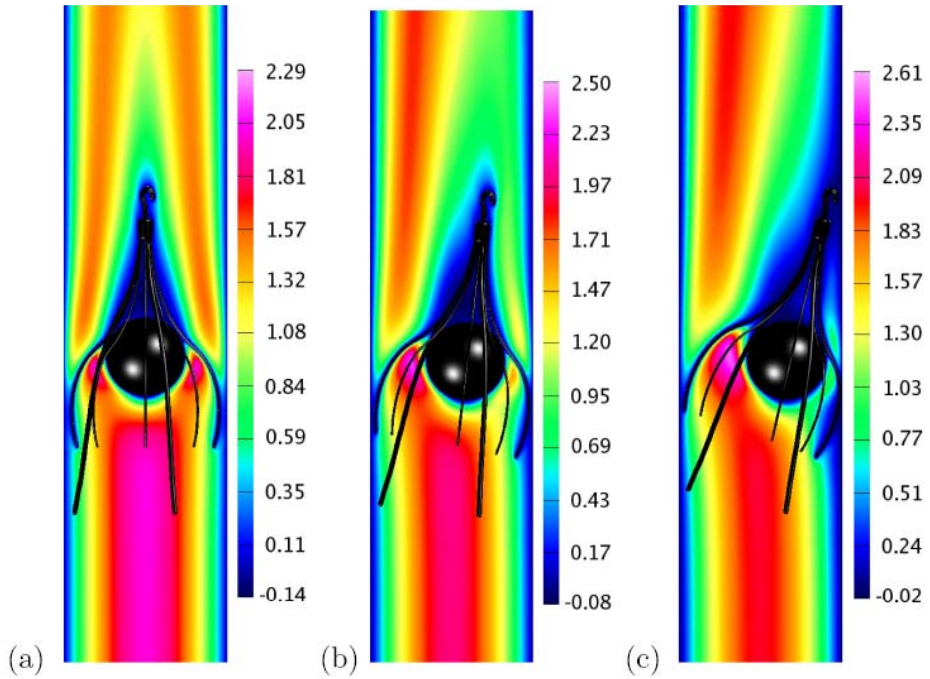

Figure 5: Axial velocity contours for the partially occluded Celect filter with a 1mL spherical clot: (a) zero-tilt; (b) half-tilt (7.5 degrees); (c) full-tilt (15 degrees).

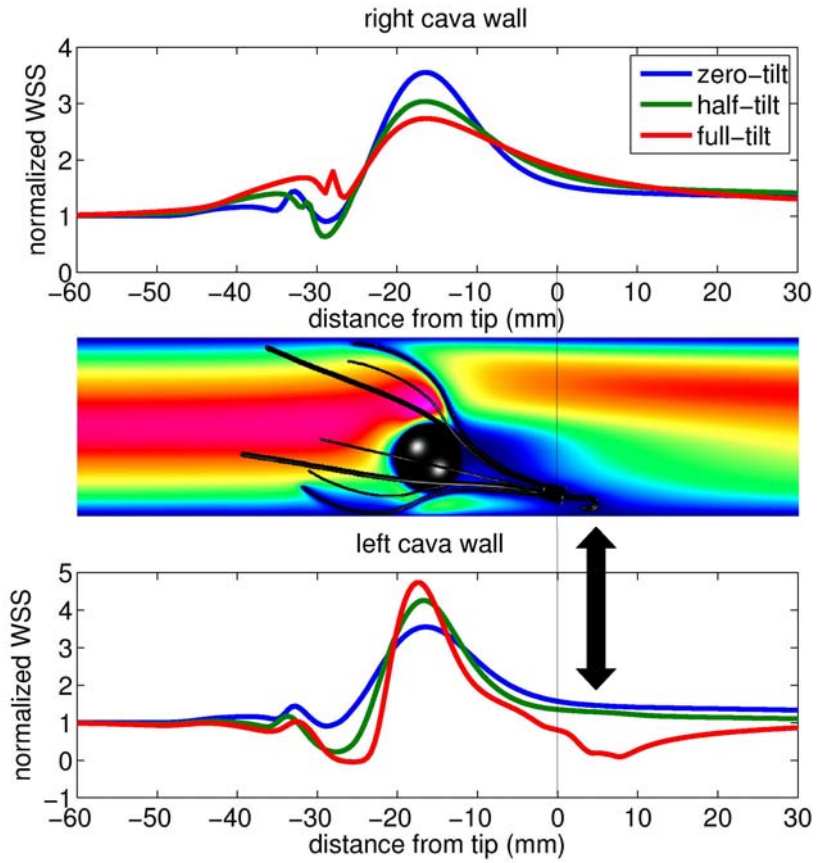

Figure 6: Wall shear stress for the partially occluded Celect filter with 0.5mL thrombus: right cava wall (top); left cava wall (bottom). The arrow highlights the correspondence between low WSS and stagnant/recirculating flow when the hook lies near the cava wall in the full-tilt position.

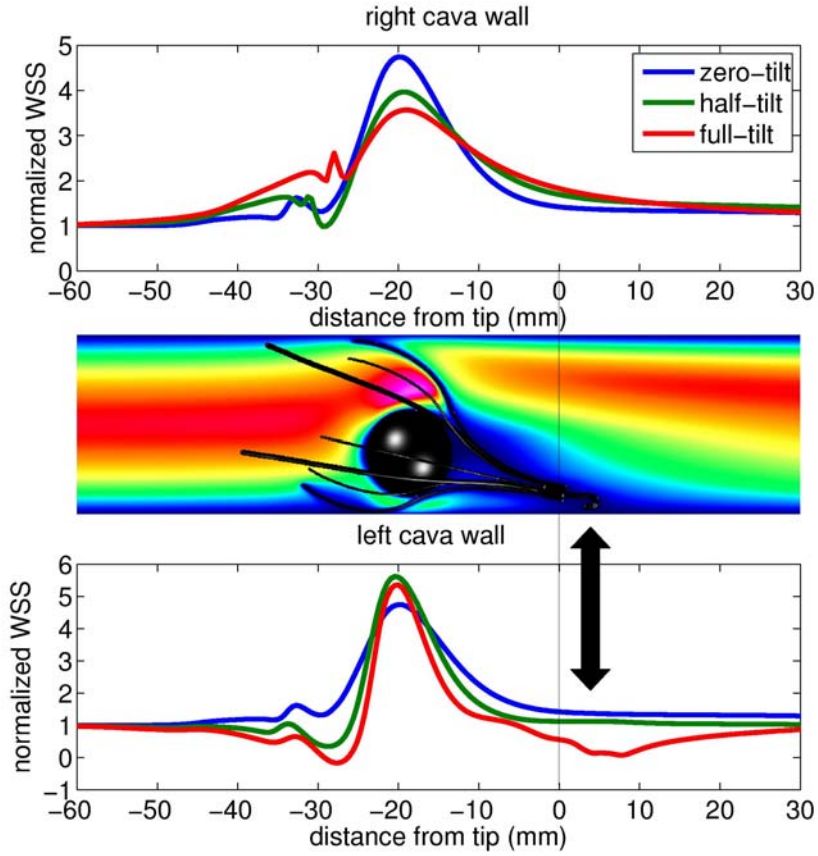

Figure 7: Wall shear stress for the partially occluded Celect filter with 1mL thrombus: right cava wall (top); left cava wall (bottom). The arrow highlights the correspondence between low WSS and stagnant/recirculating flow when the hook lies near the cava wall in the full-tilt position.